OXYGEN ISOTOPIC EVOLUTION OF THE EARLY SOLAR NEBULA AND ITS IMPLICATION FOR CHONDRITIC CONSTITUENTS. Takashi Fukui[1] and Kiyoshi Kuramoto[1], [1] *Department of Cosmoscience, Hokkaido University, Sapporo 060-0810, Japan, (ftakashi@ep.sci.hokudai.ac.jp).*

Introduction: Coexistence of the large (between CAIs and chondrules) and small (among chondrules) variations of oxygen isotopic composition in chondrites is a longstanding enigma. On an oxygen three-isotope plot [1], chondrules locate near $\delta^{17,18}\mathrm{O}_{\mathrm{SMOW}} \sim 0$ ‰ with little variation (about ± 5 ‰). In contrast, CAIs plot on a slope-1 line $\delta^{17,18}\mathrm{O}_{\mathrm{SMOW}}$ from ~ 0 to ~ -40 ‰. Measurements of Pb-Pb and Al-Mg ages of them [2–4] imply that the oxygen isotopic composition of the inner solar nebula had evolved from ^{16}O-rich (CAIs-like) to ^{17,18}O-rich (chondrules-like) one by more than 40 ‰ in ~ 1 Myr. In addition, the little isotopic variation among chondrules (and planetary materials) implies that the oxygen isotopic composition was spatially and temporally unchanged during their main formation period (1–2.5 Myr after CAIs [3,4]).

Such pattern of chondritic constituents suggests the existence of ^{16}O-rich and ^{17,18}O-rich reservoirs, and mechanical mixing of them in the solar nebula. Yurimoto and Kuramoto (2004, hereafter YK04) [5] have applied an enrichment process of vaporized species due to radial gas-dust fractionation [6] to ^{17,18}O-rich H_2O originated in the parent molecular cloud, and given an explanation for the isotopic heterogeneity between CAIs and chondrules. However, the time and spatial variations of the nebula oxygen isotopic composition are poorly revealed because their calculation was limited to the quasi-steady states for CTTS and WTTS stages.

In this study, we improve the YK04 model to simulate the time-dependent isotopic evolution of the solar nebula, and perform advanced comparisons with the isotopic composition and chronology of CAIs and chondrules. A detailed simulation on the H_2O enrichment process has already been presented by Ciesla and Cuzzi (2006) [7]. In their model, the enrichment is mainly caused by m-size boulders, which migrate inward fastest. However, even mm- or cm-size particles are capable of concentrating the oxygen reservoirs severalfold [5]. In addition, the ubiquitous occurrence of chondrules in primitive meteorites seems to imply that their formation had mainly occurred before large bodies occupied dominant mass fraction of solid material. Thus our interest is the epoch before the formation of the boulders and planetesimals.

Model: We solve advection-diffusion equations for the reservoirs in both gas and solid phases;

$$\frac{\partial C_{i,\mathrm{g}}}{\partial t} + v_{\mathrm{g}}\frac{\partial C_{i,\mathrm{g}}}{\partial r} - \frac{1}{r\Sigma_{\mathrm{g}}}\frac{\partial}{\partial r}\left[rD\Sigma_{\mathrm{g}}\frac{\partial C_{i,\mathrm{g}}}{\partial r}\right] = S_{\mathrm{subl},i} - S_{\mathrm{cond},i}\ ,$$

$$\frac{\partial C_{i,\mathrm{d}}}{\partial t} + v_{\mathrm{d}}\frac{\partial C_{i,\mathrm{d}}}{\partial r} - \frac{1}{r\Sigma_{\mathrm{g}}}\frac{\partial}{\partial r}\left[rD\Sigma_{\mathrm{g}}\frac{\partial C_{i,\mathrm{d}}}{\partial r}\right] + \frac{C_{i,\mathrm{d}}}{r\Sigma_{\mathrm{g}}}\frac{\partial}{\partial r}[r\Sigma_{\mathrm{g}}(v_{\mathrm{d}} - v_{\mathrm{g}})] = -S_{\mathrm{subl},i} + S_{\mathrm{cond},i}\ ,$$

where t is time, r is the distance from the center, C_i is the concentration of species i (silicate and H_2O), $S_{\mathrm{subl},i}$ and $S_{\mathrm{cond},i}$ are the source/sink due to sublimation and condensation, Σ_{g}, v_{g} and D are the column density, radial velocity and turbulent diffusivity of the nebula gas and v_{d} is the radial velocity of dust particles, respectively. Difference between v_{g} and v_{d} causes "traffic jam" at the sublimation fronts of the reservoirs, which result in the enrichment of them.

Disk model. According to the observations of T Tauri disks [8,9], the mass accretion rate is given by $\dot{M}(t) \sim 10^{-8} \times (t/10^6\ \mathrm{yr})^{-1.5}\ M_\odot\ \mathrm{yr}^{-1}$. Our calculation begins at the time $\dot{M} = 10^{-7} M_\odot\ \mathrm{yr}^{-1}$. The nebula mass at each time is obtained from $M(t) = M_0 - \int_0^t \dot{M}(t')dt'$, where M_0 is the initial nebula mass. We simply model Σ_{g} in the form of $\Sigma_{\mathrm{g}}(t, r) = \Sigma_{\mathrm{g}}(t, 1\ \mathrm{AU}) \times (r/1\mathrm{AU})^{-p}$, where $\Sigma_{\mathrm{g}}(t, 1\ \mathrm{AU})$ is determined to satisfy $\int_{0.05\mathrm{AU}}^{r_{\mathrm{out}}} 2\pi r \Sigma_{\mathrm{g}}(r, t) dr = M(t)$ (r_{out} is the outer edges of the nebula). Then v_{g} and D are calculated by using the relation

$$\dot{M} = -2\pi r \Sigma v_{\mathrm{g}} = 3\pi \Sigma D\ ,$$

where D is assumed to be equal the turbulent viscosity ν. The midplane temperature of the nebula is determined by solving radiative transfer with simple method [7,10]. Although uncertainty in the nebula opacity might displace the location of evaporation fronts, our results are essentially unchanged.

Determination of v_{d}. Motion of dust particles in the turbulent nebula gas is described by the two-component fluid equations [11]. However, calculation of v_{d} requires the typical radius of dust particles. Assuming that larger particles occupy dominant mass fraction, the radius is represented by that of the largest particle a_{max}. We calculate a_{max} supposing that it is maintained by collisional disruption. Dust particles mainly accrete the smallest particles to grow. The collisional velocity, which is dominated by vertical dust motion, increases with size difference and collisional disruption begin to occur at the critical collisional velocity v_{crit}. This puts an upper limit on the dust particle size. Taking $v_{\mathrm{crit}} = 1\ \mathrm{m\ s}^{-1}$ [12], we obtain $a_{\mathrm{max}} \sim$ several mm at $\dot{M} \sim 10^{-8} M_\odot\ \mathrm{yr}^{-1}$. This size is consistent with that of the largest chondrules.

Partitioning of oxygen: Partitioning of oxygen, with which we translate $C_{\mathrm{H_2O}}$ and C_{silicate} into local mean oxygen isotopic composition of the nebula, is shown in Table 1. Taking the total number of oxygen equals 14, the amount of oxygen partitioned into silicate ($MgO + SiO_2$) is 3 based on the solar abundance [13]. We adopt H_2O and CO abundances and their initial isotopic fractionations after YK04 for comparison. Note that the origin of δ-values in the table is the initial solar composition. The relationship between $\delta^{17,18}\mathrm{O}_{\mathrm{solar}}$ and $\delta^{17,18}\mathrm{O}_{\mathrm{SMOW}}$ is discussed later.

Results & Discussion: Figure 1 shows the model results for $M_0 = 0.05 M_\odot$, $p = 1.0$, $r_{\mathrm{out}} = 100$ AU. It appears that the concentrations of silicate and H_2O at their sublimation fronts (where the gradient discontinuously changes) increase with time over first ~ 2 Myr. This is mainly because of the decrease of $|v_{\mathrm{g}}|$ associated with decay of the disk accretion and the increase of $|v_d|$ due to dust growth. The enriched silicate and H_2O vapors are transported inward, thus the composition inside the sublimation fronts also changes gradually. During this epoch, the enrichment of H_2O vapor inside the snow line monotonically changes the local mean oxygen isotopic composition from the initial solar to ^{17,18}O-rich one, as proposed by YK04. In addition, the isotopic evolution at the innermost region is partially inhibited owing to the enrichment of relatively ^{16}O-rich (solar) silicate. After $t \sim 2.3$ Myr, increase of the concentrations begins to decelerate, then turns into decrease, because of dust depletion outside the sublimation fronts. Until $t \sim 3.3$ Myr, the temporal variation of the isotopic composition inside the snow line is kept within ~ 10 ‰.

Next, we compare the model result with the isotopic composition and chronology of CAIs and chondrules. Chondrules would be formed at a moderately hot region between the silicate-sublimation line and the snow line. Considering that chondrules have to be formed at the time when the nebula was temporally constant in isotopic composition, their formation stage matches during $2.3 \lesssim t \lesssim 3.3$ Myr in this model run (Figure 2). In this case, the oxygen isotopic composition of chondrules ($\delta^{17,18}\mathrm{O}_{\mathrm{SMOW}} \sim 0$ ‰) becomes $\delta^{17,18}\mathrm{O}_{\mathrm{solar}} \sim 70$ ‰. During this stage, the spatial heterogeneity is also fairly small inside the snow line, which may explain the small isotopic variation among chondrules and planetary material. The chronological constraint infers the occurrence of CAIs formation at ~ 1 Myr prior to the onset of chondrules formation. Then the isotopic difference between CAIs and chondrules is expected to be ~ 40 ‰, which is consistent with the actual chondritic samples.

During the chondrules formation, the disk accretion have decayed to $\dot{M} \sim 10^{-9} M_\odot$ yr^{-1}. In this quiescent nebula, dust particles efficiently settle and concentrate at the nebula midplane [14]. If the dust layer becomes substantially thin, planetesimals are possibly formed by gravitational instability. The prior formed chondrules would accrete into their parent body at this time. CAIs, which would be formed at the innermost region of the nebula, might be circulated by bipolar flows [15] and then taken up by planetesimals.

References: [1] Clayton, R. N. (1993) *Ann. Rev. Earth Planet. Sci* 21, 115–149. [2] Amelin, Y. et al. (2002) *Science* 297, 1678–1683. [3] Kita, N. T. et al. (2000) *GCA* 64, 3913–3922. [4] Kurahashi, E. et al. (2004) *LPSC XXXV*, #1476. [5] Yurimoto, H. and Kuramoto, K. (2004) *Science* 305, 1763–1766. [6] Cuzzi, J. N. and Zahnle, K. (2004) *ApJ* 614, 490–496. [7] Ciesla, F. and Cuzzi, J. N. (2006) *Icarus* 181, 178–204. [8] Calvet, N. et al. (2000) in *Protostars and Planets IV*, 377–399. [9] Hartmann, L. (2005) in *Chondrites and the Protoplanetary Disk*, 131–144. [10] Cassen, P. (1994) *Icarus* 112, 405–429. [11] Nakagawa, Y. et al. (1986) *Icarus* 67, 375–390. [12] Dominik, C. et al. (2007) in *Protostars and Planets V*, in press. [13] Lodders, K. (2003) *ApJ* 591, 1220–1247. [14] Miyake, K. and Nakagawa, Y. (1995) *ApJ* 441, 361–384. [15] Shu, F. H. et. al. (1996) *Science* 271, 1545–1552.

Table 1: Partitioning of O

Property/Reservoir	Silicate	H_2O	CO
sublimation point (K)	1350	160	-
O (total = 14)	3	5	6
$\delta^{17,18}\mathrm{O}_{\mathrm{solar}}$	0	+120	-100

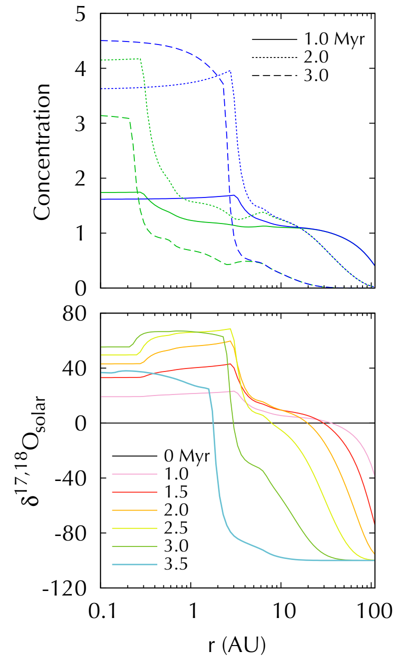

Figure 1: Evolution of the concentrations of total silicate and H_2O in gas and solid phases (top) and the local mean oxygen isotopic composition (bottom) in the solar nebula. In the top panel, the green and blue lines represent the concentration of silicate and H_2O, respectively.

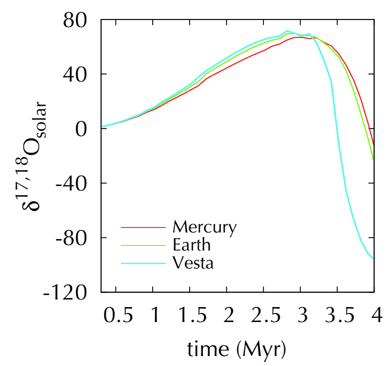

Figure 2: Time variation of the local mean isotopic composition at the present orbits of Mercury, Earth and Vesta.